Pulse Shaping for Multicarrier Modulation in Doubly Dispersive Channels

by
Anil Pandey

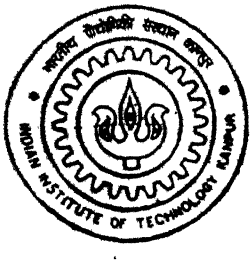

DEPARTMENT OF ELECTRICAL ENGINEERING
Indian Institute of Technology Kanpur
March, 2001

Pulse Shaping for Multicarrier Modulation in Doubly Dispersive Channels

A Thesis Submitted
in Partial Fulfillment of the Requirements
for the Degree of

Master of Technology

by

Anil Pandey

to the

Department of Electrical Engineering
Indian Institute of Technology, Kanpur

March, 2001

23-3-2001

Certificate

This is to certify that the work contained in the thesis entitled "*Pulse Shaping for Multicarrier Modulation in Doubly Dispersive Channels*", by *Anil Pandey*, Roll No. 9910411 has been carried out under my supervision and that this work has not been submitted elsewhere for a degree.

March, 2001

A. K. Chaturvedi
Assistant Professor,
Department of Electrical Engineering,
Indian Institute of Technology,
Kanpur.

Acknowledgements

First of all I would like to express my deep regards and indebtedness to my thesis supervisor Dr. A. K. Chaturvedi who taught me to walk and talk in the field of communication. His encouragement and constructive criticism have always been like a lamp-post in the sea. I thank him for his unlimited patience and cooperation throughout.

Sincere thanks are also due to the friends, Amit, Ajay, Ashok, Deepak, Pradeep, Raju, Sasi, Satyendra, Shahrukh, Sachin, Venu, Prabhatji, Vishwanathji and Sahuji for their cooperation and valuable help from time to time. Our discussions have always been helpful in understanding the subject properly. My special thanks go to the friends of my college days for being with me in my hard days. The moral support from my parents, brothers, sisters and other family members has also been adorable. I would also like to thank my basketball and swimming companions for providing me some light moments.

Last but not the least, it is due the blessings of the almighty without Him this humble piece of work would not have been in shape.

Anil Pandey

Abstract

Single carrier systems use equalizers to remove channel impairments. The increase of data rate increases equalizer complexity making its implementation difficult. The idea of multicarrier modulation is to transmit high rate data over many carriers by dividing it into several low rate data streams and hence making equalizer design potentially simpler. But placing many carriers in same available bandwidth gives rise to Inter Carrier Interference (ICI). To get ICI free transmission at least in ideal channel, carriers must be orthogonal to each other. Pulse shape used to represent a symbol, plays an important role in reducing ICI. But pulse shaping has a limitation that the pulse decreasing ICI makes it sensitive towards ISI. Though ICI can also be decreased by increasing carrier spacing, but it will decrease the spectral efficiency of system. Hence pulse shaping can give a compromise between ISI, ICI and spectral efficiency, in order to minimize total interference. Delay dispersion of channel gives rise to ISI and doppler dispersion to ICI. Hence pulse design should also depend upon the channel characteristics in which it has to be used. In this thesis pulse shaping issues have been considered and orthogonal as well as non-orthogonal pulses have been compared for doubly dispersive channels.

Contents

List of Figures

Chapter 1

Introduction

With the spectacular growth in communication facilities, the demand for higher data rates is increasing day by day. Most communication techniques use single carrier modulation to transmit data, which needs complicated equalizer blocks at the receiver to nullify the impairment made by the channel. Though almost no communication system runs without equalizers, but we always try to minimize their need as they are complicated blocks. Normally more is the data rate, more complicated the equalizer is. This gave rise to the idea of transmitting high speed data occupying large bandwidth by dividing into several low speed data streams occupying smaller bandwidth. To do so we transmit many data streams on frequency division multiplexed subcarriers. Hence the equalizer needed becomes less complicated and sometimes it is completely eliminated. The systems based on this idea are put under the family of multicarrier systems.

1.1 Few implementations of multicarrier systems

The principle of multicarrier was originally applied in Collins' Kineplex Systems in [4]. There are claims of even early implementations. It has since been called by many names and used with varying degree of success in different media, e.g.[8]

- FDM telephony group band modem.
- Telephony voice band modem.
- Upstream cable modem.

- Digital audio broadcast (DAB).
- Digital video broadcast (DVB)

Performance of multicarrier systems widely varies depending upon the application.

1.2 Different channel conditions and multicarrier

Because of using many carriers in the same available bandwidth, multicarrier systems become more sensitive towards any doppler dispersion than single carrier systems. However, in channels having delay dispersion or non-flat response but negligible doppler dispersion, multicarrier proves to be a promising technique. Successful implementations in xDSL[1] and DAB are examples using thousands of carriers over channels having almost no doppler dispersion but delay dispersion and non-white noise due to crosstalk.

In doppler dispersive channels, multicarrier may benefit in other ways, for example by requiring an amplifier of lesser bandwidth, hence making amplifier design simpler. But normally number of carriers in such implementations is very small. In CDMA2000 it is proposed to use multicarrier for cellular communication, where doppler dispersion cannot be ignored. Additionally it gives the compatibility with IS-95 and the hardware of IS-95 can be used with little change.

1.3 Motivation for present work

Multicarrier systems have been used since long. Many of the implementations have had high degree of success. But all of them were sensitive towards doppler dispersion and hence their use was restricted to cables only. Reason behind the sensitivity to doppler dispersion is closely spaced carriers and rectangular pulse shape used which corresponds to the *sinc* spectrum having high sidelobes. Efforts have been made to reduce sidelobes by applying different pulses. Though it can work well in cables having negligible doppler dispersion but may not prove good enough in mobile environments showing both the dispersions together.

[1]Many implementations in DSL family like ADSL, HDSL, VDSL etc are collectively known as xDSL.

The motivation for this work was to study the issues and capabilities of pulse shaping and for multicarrier communication in doubly dispersive channels.

1.4 Organization of thesis

In Chapter 2 general multicarrier design and related issues have been discussed. Successful DFT based implementations of multicarrier systems have been described and problems encountered in such systems have been discussed. Chapter 3 gives the characterization and modeling of channels and then presents pulse design aspects. Few orthogonal and non-orthogonal pulses also have been given. Simulation modeling of multicarrier systems and channels used in this work is also given. Chapter 4 gives the analysis of different pulses and their comparison.

Chapter 2

Multicarrier modulation: An overview

Multicarrier modulation is a form of Frequency Division Multiplexing. It has been called with many names depending upon the implementation method. Discrete Multitone (DMT) has been popular in Digital Subscriber Loops (DSLs) and Orthogonal Frequency Division Multiplexing (OFDM) in broadcasting. Likewise other implementations are also in practice. We will proceed with the general block diagram.

2.1 General block diagram

The general block diagram has been given in Figure 2.1.

Input to serial to parallel converter (S/P) is a sequence of symbols of B bits each. The output for each symbol is N_c groups of $b(k)$ bits each. That is

$$B = \sum_{k=0}^{N_c-1} b(k) \tag{2.1}$$

The groups of b(k) are then constellation encoded, filtered and modulated onto N_c subcarriers. The output of modulators is passed through a digital to analog converter (DAC) and possibly through a low pass filter before transmission. RF up conversion may be done to translate it in allotted RF range.

Receiver is effectively the mirror image of transmitter.

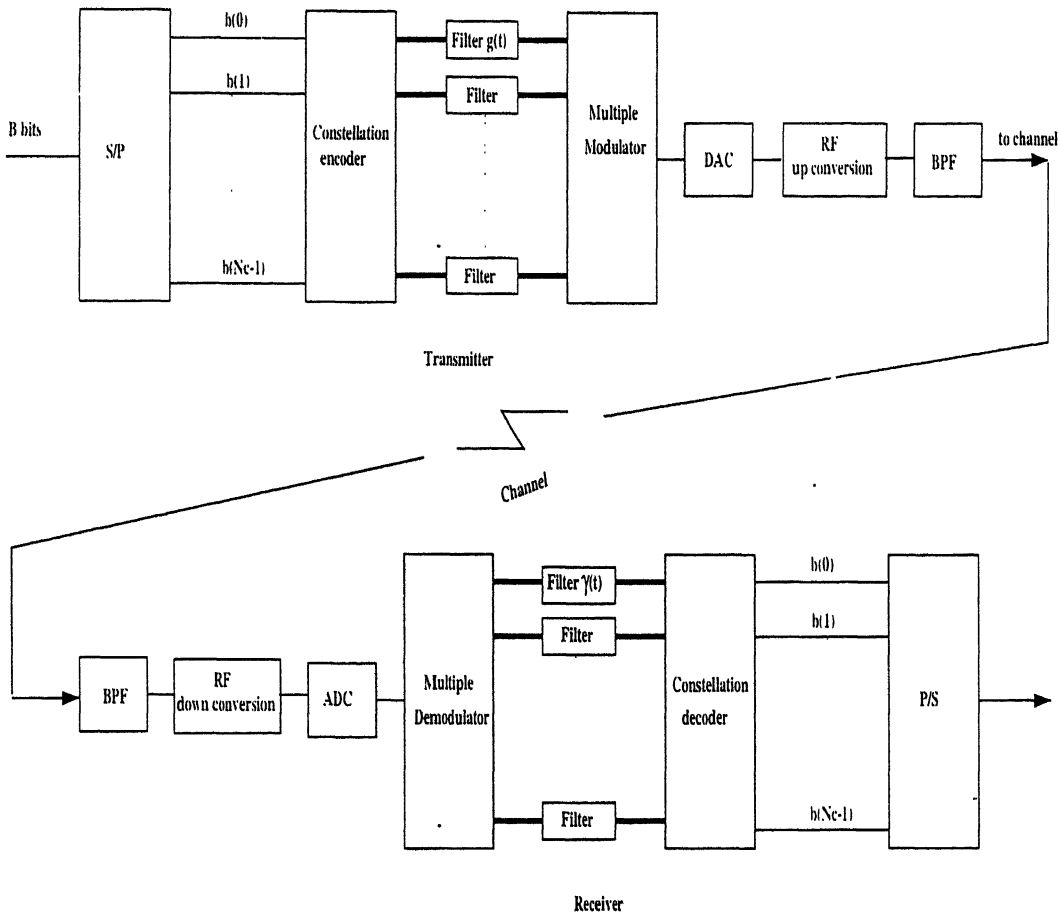

Figure 2.1: General block diagram

2.2 Subcarrier spectra and spectral efficiency

Method of dividing available transmission bandwidth for subcarriers gives rise to many implementations. The simplest way may be to divide it into disjoint frequency slots. Because of difficulty of implementation[1] of very sharp filters each of the signal must use a bandwidth $(1+\alpha)f_s$, which is greater than the Nyquist minimum f_s [3]. Hence the efficiency of band usage is $\frac{1}{(1+\alpha)}$. The efficiency of band usage can be increased by using overlapping spectra[1] and keeping carriers orthogonal. One such implementation OFDM uses completely overlapping spectra [2]. OFDM is basically multicarrier modulation without pulse shaping. There is also a possibility of multicarrier modulation with pulse shaping [2]. Both types of systems

[1]We see another constraint on it. Even if we can implement sharp filters, it will correspond to a sinc pulse shape, which will be highly sensitive towards delay dispersion and timing errors. Hence this is not favorable to use it where our principle aim is to combat delay dispersion by multicarrier modulation.

viz. multicarrier without pulse shaping and multicarrier with pulse shaping have their own advantages and disadvantages. These will be discussed in detail later.

2.2.1 Spectral efficiency

The spectral efficiency can be defined as number of bits transmitted per hertz. Let Δf_c be carrier spacing in frequency and Δf be sub-carrier bandwidth. It can be visualized that for $\Delta f_c > \Delta f$, full efficiency can not be achieved because of empty frequency slots in between. For $\Delta f_c \leq \Delta f$ spectral efficiency ρ can be formulated as[5],

$$\rho = \frac{1}{\frac{N_c - 1}{N_c}\Delta f_c T_s + \frac{\Delta f T_s}{N_c}} \qquad symbols/Hz \tag{2.2}$$

Now if we use $\Delta f_c T_s = 1$ and $N_c \gg 1$, we can approach maximum efficiency as $\rho \simeq 1$.

2.3 Maximum achievable bit rate

The performance of a data transmission system is usually analyzed and measured in terms of the probability of error at a given bit rate and signal to noise ratio (SNR). The variables for multicarrier signal are number of bits per symbol m_n, and the proportion γ_n of the total transmitted power P, that is alloted to each sub band. The aggregate bit rate is approximately maximized if these variables are chosen such that the bit error rates in all the sub bands are equal [3]. In order to calculate attainable bit rate for a channel with the transfer function $H(f)$ and noise power spectrum at the input to the receiver $U(f)$. We can approximate $H(f)$ and $U(f)$ by segments H_n and U_n centered about carrier frequency $f_{c,n}$, defined as,

$$f_{c,n} = n\Delta f_c \qquad \text{for } n_1 \leq n \leq n_2 \tag{2.3}$$

The possible non whiteness of the noise should be noticed which is discussed later. Probability of bit error for QAM in any band, assuming no interference from other bands is[7]

$$P_n = 4Q\left[\frac{3m_n E_{av}}{(2^{m_n} - 1)N_0}\right]^{\frac{1}{2}} \tag{2.4}$$

where E_{av} is average bit energy received. Hence $m_n E_{av}$ is average symbol energy received. Total power transmitted is P and the fraction alloted to n^{th} sub-band is γ_n. Channel transfer

function is H_n. Hence power received for n^{th} sub-band is $\gamma_n P|H_n|^2$. Noise power spectral density for n^{th} sub-band is U_n. Hence replacing $m_n E_{av}$ by $\gamma_n P|H_n|^2$ and N_0 by U_n.

$$P_n = 4Q\left[\frac{3\gamma_n P|H_n|^2}{(2^{m_n}-1)U_n}\right]^{\frac{1}{2}} \tag{2.5}$$

Thus the total number of bits that can be transmitted in one symbol with error probability $\mathcal{P}$ using N_c sub bands can be written as,

$$M = \sum_{n=0}^{N_c-1} log_2\left[1 + \frac{3}{[Q^{-1}(\mathcal{P}/4)]^2}\frac{\gamma_n P|H_n|^2}{U_n}\right] \tag{2.6}$$

where $\sum_{n=0}^{N_c-1}\gamma_n = 1$. The most efficient use of the channel is made if the symbol rate f_s is made equal to the carrier separation Δf and both are made very small. Then the summation of equation 2.6 can be approximated by an integration, and the maximum bit rate,

$$R = \int_{f_l}^{f_u} log_2\left[1 + \frac{3}{[Q^{-1}(\mathcal{P}/4)]^2}\frac{P|H_f|^2}{WU_f}\right] df \tag{2.7}$$

where f_l and f_u denote lower and upper band edges. Equation 2.7 is very similar to the bit rate for a single-carrier QAM (SCQAM) signal equalized by a DFE[3]. It should be noted that equation 2.7 assumes that the number of bits per carrier is continuously variable but in practice, each m_n must be integer. It was found[3] that total bit rate achieved is only slightly less than that given by equation 2.7.

Thus the aggregate bit rate for multicarrier modulation is approximately equal to that for SCQAM/DFE.

2.3.1 Adaptive loading

It is intuitively clear that if the ratio $|H(f)|^2/U(f)$ varies significantly across the band, our objective of making each sub-band bit error rate P_n equal, is not fulfilled. This results in a high bit error rate. Hence we can keep on adapting the loading, i.e. changing m_n. This is called Adaptive loading, unlike previously fixed m_n in fixed loading. We will give a schematic approach to adapt m_n, given in [3].

Given a set of signal to noise ratios, measured in the receiver when the transmitter is transmitted at the maximum permitted level in all the sub-bands, calculate the terms, $\Delta P_{m,n} = P_{m,n} - P_{m-1,n}$, where $P_{m,n}$ is the transmit power needed in the sub-band n to transfer m bits per symbol at some predefined error rate.

Then assign bits one at a time to carriers, each time choosing the carrier that requires the least incremental power. This can be described as follows,

- Search row 1 for the smallest $\Delta P_{i,n}$
- Assign one or more bits to sub band n
- Incremental M and P_{tot}, that is, $M' = M + 1$ and $P_{tot} = P_{tot} + \Delta P_{i,n}$
- Move all terms of column n up one place, that is $\Delta P'_{i,n} = \Delta P'_{i+1,n}$
- Repeat search

The process stops when P_{tot} reaches the maximum available power or the total bit rate reaches the maximum allowable bit rate, depending upon the mode of operation. All allotted powers must be scaled to adjust P_{tot} to the correct value.

2.4 Crosstalk

A dominant impairment in multicarrier systems is strongly correlated, *Crosstalk*. Two commonly known terms for its characterizations, near end crosstalk (NEXT) and far end crosstalk (FEXT), have originated from DSL systems[8], but can be experienced in any multicarrier system. Interferences continuing in the same direction as the interfering signal, add up to form *far end crosstalk (FEXT)* and those come back toward the source of the interferer, add up to form *near end crosstalk (NEXT)*. If both NEXT and FEXT can occur in a multicarrier system, NEXT will in general be more severe. NEXT increases with frequency and at VDSL frequencies (upto 15 MHz) it would be intolerable. Therefore, VDSL systems are specially designed to avoid it altogether.

2.5 Peak to average power ratio

A multicarrier signal consists of a number of independently modulated subcarriers which can give a large peak to average power ratio (PAPR) when added up coherently. When N signals are added with the same phase, they produce peak power that is N times the average

power. The peak power is defined as the power of a sine wave with an amplitude equal to the maximum envelope value[9]. An alternative measure of the envelope variation of a signal is *Crest Factor*, which is defined as the maximum signal value divided by the root mean square (rms) signal value. A large PAPR brings disadvantages e.g. an increased complexity or more quantization noise in analog to digital and digital to analog converters and a reduced efficiency of the RF amplifier.

2.5.1 PAPR Reduction Techniques

Several techniques proposed to reduce PAPR can be divided into three categories.

- **Signal distorting techniques-** These techniques reduce the peak amplitude simply by non-linearly distorting the multicarrier signal e.g. clipping high amplitudes. Examples of three techniques are peak windowing and peak cancellation.
- **Coding techniques-** Simple forward error correcting codes can be used, which exclude multicarrier symbols with a large PAPR.
- **Scrambling techniques-** PAPR can also be reduced by the scrambling of multicarrier signal with different scrambling sequences and selecting which gives the smallest PAPR.

2.6 Constraints on number of subcarriers

Our original idea to use multicarrier modulation is to transmit high data rate signal by dividing it into low data rate signal and transmitting on several subcarriers. But we can not keep on increasing number of carriers indefinitely. Certain constraints on maximum number of carriers can be listed as follows-

- **Peak to average power ratio-** which is proportional to the number of carriers and we can not handle PAPR more than a limit.
- **Increasing sensitivity to frequency dispersion.**

- **Latency**[2]- This will be proportional to the symbol duration and hence to the number of subcarriers as well. We must limit the symbol duration to meet the requirement of maximum allowable latency.

- **Difficulty in implementation of large filter banks.**

2.7 Multicarrier system design issues

After an overall look to multicarrier systems, we find following issues related to multicarrier systems.

- Number of subcarriers and optimum subchannel bandwidth.
- Constellation design and adaptive loading,
- Pulse shape design.
- Synchronization.
- Peak to average power reduction.

The most successful implementations of multicarrier till now are DFT based systems. DMT and OFDM are such successful implementations.

2.8 DFT based multicarrier systems

For a large number of carriers, the array of sinusoidal generators and coherent demodulators required in multicarrier system becomes unreasonably expensive and complex. We find a simplest way[2] of performing multicarrier modulation shown in figure 2.2 setting $g(t) = 1$ and using QAM constellation. Suppose number of subcarriers is N_c, modulated at the frequencies $f_0, f_1, \ldots\ldots f_{N_c-1}$. Frequency separation between adjacent carriers is Δf_c. Assuming n^{th} symbol as $(a_n + jb_n)$ the output of QAM modulator will be $y_n(t) = (a_n cos 2\pi f_n t + jb_n sin 2\pi f_n t)$.

[2]Typical name given to the processing delay.

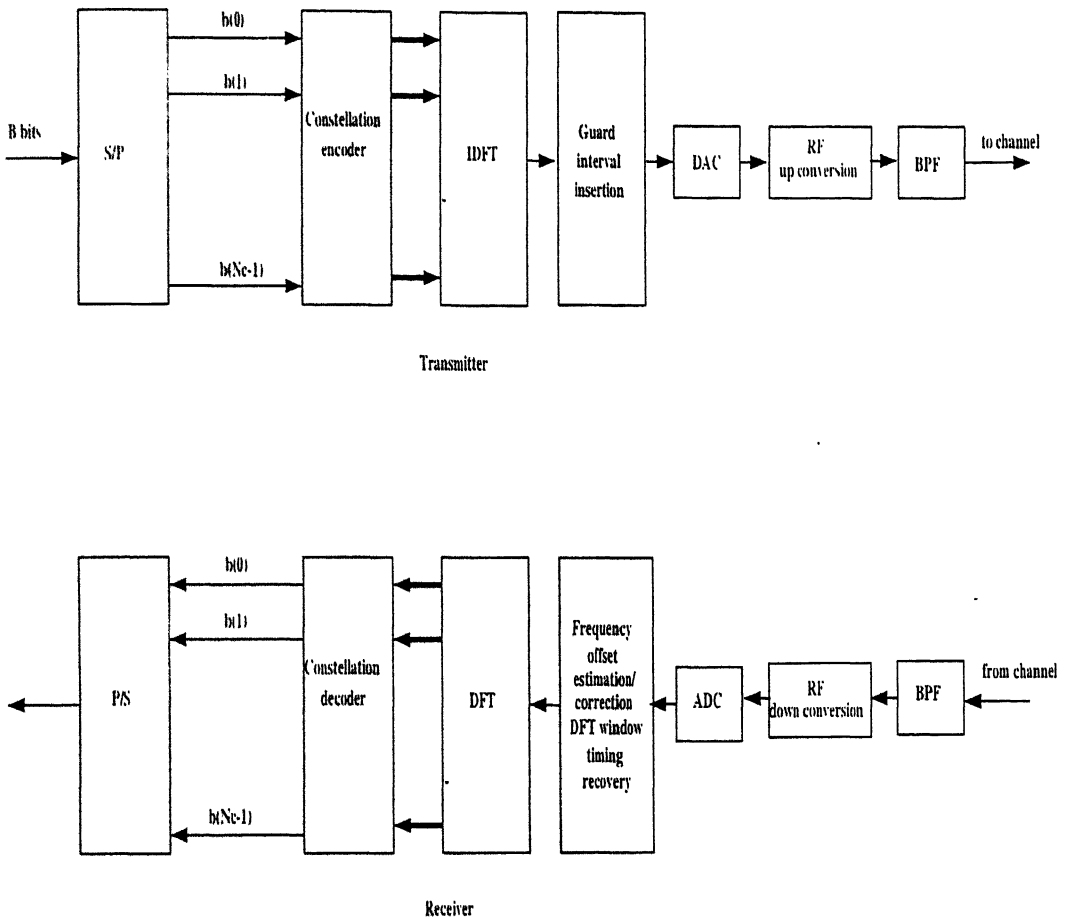

Figure 2.2: General block diagram of DFT based multicarrier system.

Denoting $c_n = (a_n + jb_n)$, we can write QAM modulator output as $y_n(t) = c_n e^{j(2\pi f_n t)}$. Hence the signal transmitted to the channel, for a multicarrier system using N_c carriers is.

$$y(t) = \sum_{n=0}^{N_c-1} c_n e^{j(2\pi f_n t)} \tag{2.8}$$

where $c_n(t)$ is QAM symbol transmitted at n^{th} carrier at time t. Assuming carrier spacing $\Delta f_c = \frac{1}{T}$, the condition for maximum spectral efficiency, $f_n = n\Delta f_c = \frac{n}{T}$. $y(t)$ modifies like this,

$$y(t) = \sum_{n=0}^{N_c-1} c_n e^{(\frac{j2\pi nt}{T})} \tag{2.9}$$

If we see above equation in discrete domain, it is nothing but IDFT of the symbols transmitted.

$$y(k) = \sum_{n=0}^{N_c-1} c_{nk} e^{(\frac{j2\pi nk}{T})} \tag{2.10}$$

where $c_n(k)$ is QAM symbol transmitted at n^{th} carrier at k^{th} instant of time.

We can see the output of modulator as inverse discrete Fourier transform (IDFT) of QAM coefficient c_ns. Hence the modulator/demodulator bank can be easily replaced by a N_c point IDFT/DFT. Further for the sake of computational efficiency it can easily be implemented by its computationally efficient algorithm, Fast Fourier Transform (FFT). We should notice that though **in practice we use IDFT at the transmitter and DFT at the receiver, still there is no technical constraint on it. We can use either of one any where, or even same (DFT or IDFT) at both the ends**[2]. Using DFT at transmitter and IDFT at receiver can be simply understood that both the transformations cancel each other. It does not matter which one is done earlier. The recovery of signal by using same transformation at both the places can be explained by the duality property of fourier transform that, if, $g(t) \rightleftharpoons G(f)$, then

$$g(f) \rightleftharpoons G(-t) \tag{2.11}$$

where $\rightleftharpoons$ represents fourier transform pairs. In the discrete domain if symbols $s(k)$'s are to be transmitted as $z(n)$'s after DFT i.e.

$$s(k) \rightleftharpoons z(n) \tag{2.12}$$

then if IDFT is used at the receiver,

$$output = F^{-1}(z(n)) = s(k) \tag{2.13}$$

If DFT is used at the receiver,

$$output = F(z(n)) = s(-k) \tag{2.14}$$

We can see that in both cases signal can be recovered.

With the implementation of modulator/demodulator banks by IFFT/FFT an additional condition is imposed that total number of carriers must be such that $N_c = 2^n$, where n is an integer. In nut shell such systems are multicarrier systems with following constraints,

- $g(t) = 1$ i.e. rectangular pulse shape.
- Carrier spacing $\Delta f_c = \frac{1}{T}$
- Number of carriers $N_c = 2^n$, such that n is integer.

- Using QAM constellation.

As above systems use QAM constellation, we can give them a generic name as MQASK[8]. Most popular implementations of MQASK are DMT in DSL and OFDM for wireless uses (primarily for broadcasting). We can see for $g(t) = 1$, i.e. rectangular pulse shape, if carriers are spaced by $\frac{1}{T}$ and $f_n = \frac{n}{T}$, every carrier has integral number of cycles in one symbol duration. This way carriers will be orthogonal to each other, hence the name Orthogonal frequency division multiplexing (OFDM) comes. It is has been said in [9] and [6] that orthogonality is achieved because the spectrum of other carriers is zero at one's peak, which is not a proper reason behind orthogonality. We can find situations where above condition is not fulfilled, still we achieve orthogonality.

2.8.1 Guard Interval

Orthogonality is achieved by putting integral number of cycles in one symbol period. If because of channel impairments such as delay dispersion, this condition is lost, then along with inter symbol interference(ISI), an inter carrier interference(ICI) or crosstalk will appear. As DFT based multicarrier systems are primarily meant for the channels having delay dispersion, we can not ignore this situation. To combat it a guard period was first used in Telebit's trailblazer voiceband modem[8]. Introducing a guard interval we ensure that delayed replicas of MQASK signal have integer number of cycles as long as delay is smaller than Guard interval. Hence we simply eliminate ICI and ISI discarding the guard interval at receiver. Guard interval can be inserted in three ways,

- *Cyclic Prefix*: Add the last ν samples to the beginning of the signal and then delay collecting the samples in the receiver until the transient response has finished.

- *Cyclic Suffix*: Add the first ν samples to the beginning of the signal and then delay collecting the samples in the receiver until the transient response has finished.

- Quiet period: Use a quiet period between symbols and in the receiver add the last ν samples to the first.

There is no fundamental difference between first two techniques except a phase difference of $2\pi n\nu/N$ in carriers.

This can be seen that symbol length T_s is increased to $T_s(1+\Delta T_s)$. Hence carrier spectra are not zero at other carrier's peaks. Still we achieve orthogonality.

ISI and ICI have been easily removed or at least minimized by guard interval insertion. The price we pay for it is spectral efficiency, which is reduced to $\frac{T_s}{T_s+\Delta T_s}$ now. This may not be so significant for large number of carriers. We can always use a smaller guard interval and remove remaining ISI and ICI by equalization. Hence length of the guard interval is a compromise between efficiency and ease of designing equalizer.

2.8.2 Spectral Efficiency

Spectral efficiency achieved by DFT based multicarrier systems can be evaluated by equation 2.2 putting $\Delta f_c T_s = 1+\Delta T_s$ and can be seen that for large number of carrier it achieves almost full efficiency.

2.8.3 Sidelobe Problem

Physically realizable signals cannot be bandwidth restricted. Hence they have the frequency contents outside the band of interest also. In multicarrier systems if carriers are separated by Δf_c then for any carrier centered around f_n, the band of interest is $f_n - \frac{\Delta f_c}{2} \leq f \leq f_n + \frac{\Delta f_c}{2}$. Frequency components of the signal on this carrier, which are outside this band constitute to the *Sidelobes*. Because of the use if rectangular pulse shape the sidelobes of an MQASK modulator or demodulator fall of very slowly. Consequences are smearing the input noise in one subchannel over many. If noise in one subchannel is considerably higher than others, it may contribute to other channels as well. Hence if the subchannels have same SNRs then this noise smearing does not effect much. But if the subchannels have considerable different SNRs then one having higher SNR will loose from its capacity.

This problem can be reduced by-

- Increasing the size of FFT (i.e. reducing Δf effectively) reduces the magnitude of all sidelobes.
- A guard period allows for a very wide choice of shortened impulse responses and in doing greatly simplifies the design of equalizer. This reduces noise enhancement in

equalizers.

- Using a different modulator/demodulator which attenuates the sidelobes much more rapidly.

Chapter 3

Pulse shaping

DFT based systems discussed in last chapter have a common problem of high sidelobes because of the rectangular pulse shape used. Until channel creates any dispersion, sidelobes have no effect because of orthogonal carriers. But in doppler dispersive channels, carriers loose their orthogonality which results in inter carrier interference (ICI). ICI obviously depends upon sidelobes. Higher the sidelobes, higher the ICI will be. Few techniques have been developed to reduce sidelobes. But reducing sidelobes may result in other problems which are pronounced in other channels. So before discussing those techniques, characterization of channels must be seen.

3.1 Characterization of communication channels

Various communication channels can be put in two major categories-

1. **Time invariant:** Channels whose impulse response does not vary with time are said to be time invariant. Their impulse response can be represented as $h(t)$. Cables are examples of such channels.

2. **Time variant:** Channels whose impulse response varies with time are said to be time variant. Their impulse response can be represented as $h(t;\tau)$. Wireless channels are examples of such channels.

3.1.1 Fading channels

Mobile communication through wireless channels experiences many random impairments such as multipath and shadowing. All these impairments may collectively be experienced as fluctuation in amplitude as well as in phase and are known as *fading*. It can be modeled as a multiplicative noise i.e. a complex gaussian random variable($\alpha e^{j\theta}$) is multiplied with the signal as a result of fading. For all the fading models θ is considered to be uniformly distributed between $(0, 2\pi)$. α may be Rayleigh, Rician or Nakagami-m distributed depending upon the channel. Different names given to fading channels e.g. Rayleigh, Rician or Nakagami-m come from the distribution of α.

Coherence Time: Coherence time τ_c indicates the minimum time separation at which the correlation of fadings at the two time instants falls below a predefined value. This value may be 0.5, $\frac{1}{e}$ or 0.1 depending upon the robustness of the receiver. Maximum doppler spread (f_d) is proportional to the inverse of coherence time($\frac{1}{\tau_c}$). In fact $f_d \approx \frac{1}{\tau_c}$.

Coherence Bandwidth: Coherence bandwidth B_c indicates the minimum frequency separation at which the correlation of fadings of two frequency components falls below a predefined value. This value may again be 0.5, $\frac{1}{e}$ or 0.1 depending upon the robustness of the receiver. Maximum delay spread (τ_m) is proportional to the inverse of coherence bandwidth($\frac{1}{B_c}$). In fact $\tau_m \approx \frac{1}{B_c}$.

Depending upon the coherence time and coherence bandwidth channel can be further characterized as to be slow fading, fast fading, frequency selective or non-selective fading, delay dispersive, doppler dispersive or doubly dispersive.

- **Slow and Fast fading channels:** If symbol duration $T_s \gg \tau_c$ i.e. variation of channel is very slow compared to the symbol duration, then channel is called as slow fading channel, otherwise it is fast fading channel. Obviously this depends not only on the channel but also on the data rate.

- **Frequency non-selective(flat) and frequency selective fading channels:** If transmission bandwidth $B_s \ll B_c$ i.e. variation of channel is highly correlated for every frequency component of signal, then channel is called as frequency non-selective or flat fading channel, otherwise it is frequency selective fading channel.

3.1.2 Dispersive channels and their modeling

Sometimes channels may show dispersion in time or in frequency or in both. Depending upon the dispersion introduced by channel, dispersive channels can be characterized as-

3.1.2.1 Delay dispersive channels

If signal duration at the output of the channel is different than at the input, channel is called as delay dispersive. This phenomenon can be experienced in both fading or non-fading channels. In fading channels maximum delay, $\tau_m \approx \frac{1}{B_c}$.

In most of the practical channels delay dispersion is exponentially distributed or at least can be approximated to exponential. Hence power-delay profile is normally modeled as exponential[15] i.e. power of n^{th} path P_n delayed by T_d is $P_0 e^{\frac{-(T_d - T_0)}{\tau_{max}}}$. where T_0 is the delay of earliest reaching path. P_0 is the power of a path coming with T_0 delay.

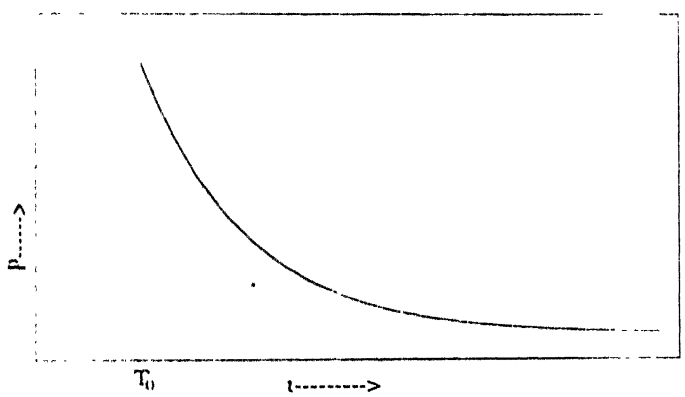

Figure 3.1: Exponential Power-delay profile

3.1.2.2 Doppler dispersive channels

If bandwidth of the signal at the output of the channel is different than at the input of it, channel is called as doppler dispersive. In fading channels maximum doppler spread, $f_d \approx \frac{1}{T_c}$.

Doppler dispersion can be modeled in a various ways. This can be Uniform, Gaussian, Rician or Jakes spectrum. Rician is suggested for rural areas as it takes a direct path in consideration. For urban environment Jakes is said to be most suitable model[11]. Power

spectral density of dispersion in this modeled is considered as-

$$S_d(f) = \frac{K}{\sqrt{1-(\frac{f}{f_d})^2}}; -f_d \leq f \leq f_d \tag{3.1}$$

where $f_d = \frac{v}{\lambda}$ is maximum doppler dispersion, v is the vehicle speed in meters per second and λ is the wavelength of signal.

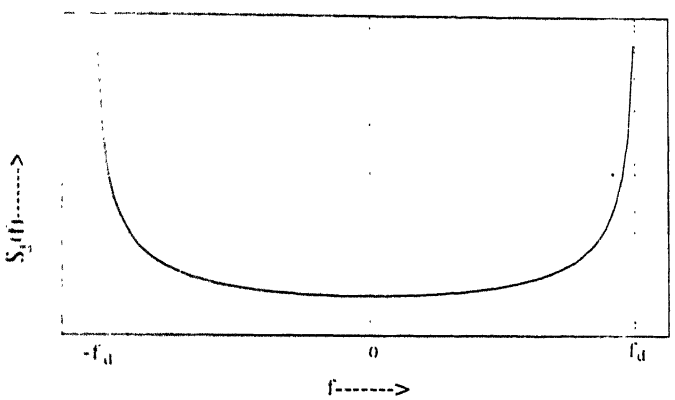

Figure 3.2: Jakes Spectrum

3.1.2.3 Doubly dispersive channels

The channels exhibiting both the delay and the doppler dispersions are called as doubly dispersive. As delay dispersion is modeled as exponential and doppler dispersion is modeled by Jakes spectrum, doubly dispersive channels are modeled as exponential/Jakes, i.e. exponential power-delay profile and Jakes doppler dispersion spectrum.

In general one can say that all the channels are doubly dispersive in nature and show delay dispersion of approximately $\frac{1}{B_c}$ and doppler dispersion of approximately $\frac{1}{\tau_c}$. But according to the signal to be transmitted, one or more properties of channel may be of interest. For example a channel may not be treated as delay dispersive if symbol duration is too large in comparison to the delay dispersion experienced in channel. The same channel may be giving severe delay dispersion for another signal having very small symbol duration.

Now with a brief digression, bit error rate in slow and frequency non-selective Rayleigh fading channels will be discussed.

3.1.3 Rayleigh Fading channels

A typical model for fading in mobile channels is Rayleigh fading. As discussed earlier, fading is modeled as a complex gaussian multiplicative noise $\alpha e^{j\theta}$, where θ is uniformly distributed between $(0, 2\pi)$. The channel is said to be Rayleigh fading if α is Rayleigh distributed, i.e. probability density function of α,

$$p(\alpha) = \frac{\alpha}{\sigma^2} e^{-\frac{\alpha^2}{2\sigma^2}} \tag{3.2}$$

where σ is a constant. Under the assumption of perfect carrier phase recovery it is assumed that BER is effected only by envelope fluctuations.

3.1.4 Bit Error rate in fading channels

In an AWGN channel bit error rate is given in terms of signal to noise ratio, $\gamma_b = \frac{E_b}{N_0}$. For fading channels γ_b is transformed to $\frac{\alpha^2 E_b}{N_0}$, with the assumption of perfect carrier recovery and slow fading. Then,

$$\mathcal{P}_{awgn}(\gamma_b) = \mathcal{P}_{fading}(\gamma_b | \alpha = 1) \tag{3.3}$$

Hence,

$$\begin{aligned} \mathcal{P}_{fading}(\gamma_b) &= \int_0^\infty \mathcal{P}_{fading}(\gamma_b | \alpha = 1) . p(\gamma_b) d\gamma_b \\ &= \int_0^\infty \mathcal{P}_{awgn}(\gamma_b) . p(\gamma_b) d\gamma_b \end{aligned} \tag{3.4}$$

Solving equation 3.4 for BPSK gives following BER expression for BPSK in Rayleigh fading[1] channel [7]

$$\mathcal{P}_{rayleigh}^{BPSK} = \frac{1}{2}\left(1 - \sqrt{\frac{\frac{E_b}{N_0}}{\frac{1}{2\sigma^2} + \frac{E_b}{N_0}}}\right) \tag{3.5}$$

where $(2 - \frac{\pi}{2})\sigma^2$ is variance of Rayleigh distribution and $\frac{N_0}{2}$ is double sided power spectral density of AWGN. It can be noticed that in the above case as the variance of fading increases, BER goes down. Comparing this BER with only AWGN case, i.e.

$$\mathcal{P}_{awgn}^{BPSK} = \frac{1}{2} erfc\left(\sqrt{\frac{E_b}{N_0}}\right) \tag{3.6}$$

[1]Rayleigh fading here means Rayleigh fading with AWGN. It is to be noted that without AWGN, Rayleigh fading will never give any error for BPSK if phase is recovered correctly.

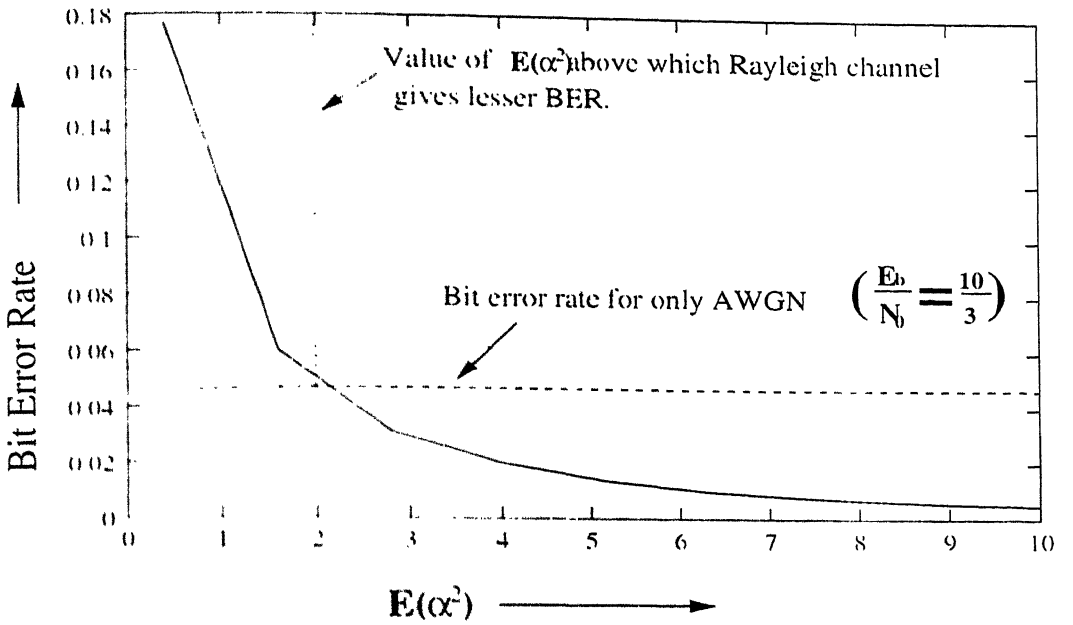

Figure 3.3: Comparison of Rayleigh and AWGN channels

It can be seen that BER in fading case lesser than only AWGN case if following inequality is satisfied.

$$E(\alpha^2) > \frac{\left(1 - erfc\sqrt{\frac{E_b}{N_0}}\right)^2}{\frac{E_b}{N_0}\left(1 - \left(1 - erfc\sqrt{\frac{E_b}{N_0}}\right)^2\right)} \tag{3.7}$$

where $E(\alpha^2) = 2\sigma^2$.

This can be seen by the simulation results given in figure 3.3. As $E(\alpha^2)$ is increased, BER is decreasing. After certain value of $E(\alpha^2)$ this BER becomes lesser than only AWGN case. It can be seen that it closely matches with the value of $E(\alpha^2)$ calculated by equation 3.7 for such situation.

Such results cannot be expected for amplitude shift keying, as envelope fluctuation itself will create errors here.

3.1.5 Modeling of doppler dispersive channels-Jakes spectrum

Various spectra has been given for modeling of doppler dispersive channels. Jakes spectrum is one which is most suitable for the modeling of urban environment. Many implementations of this spectrum are in practice. Here it has been modeled as a random doppler shift which is Jakes distributed. Hence the generation of Jakes distributed number is being discussed.

Probability density function of Jakes distributed random number y is,

$$p(y) = \frac{1}{\sqrt{1-(\frac{y}{f_d})^2}} \tag{3.8}$$

To generate it from a uniformly distributed random number x, relation between x and y can be obtained in following way. Probability density function of x is,

$$p(x) = k \qquad \text{for } 0 \leq x \leq \frac{1}{k} \tag{3.9}$$

Knowing the relation,

$$p(y) = \frac{p(x)}{\frac{dy}{dx}|_{x=f^{-1}(y)}} \tag{3.10}$$

Putting $p(x)$ and $p(y)$ here,

$$\frac{dy}{dx}|_{x=f^{-1}(y)} = k\sqrt{1-(\frac{y}{f_d})^2} \tag{3.11}$$

Solving,

$$\int \frac{1}{\sqrt{1-(\frac{y}{f_d})^2}} dy = \int k dx \tag{3.12}$$

$$f_d sin^{-1}\frac{y}{f_d} = kx \tag{3.13}$$

The relation between x, a uniform distributed random number between $(0, \frac{1}{k})$ and y, a Jakes distributed random number between $(0, f_d)$ comes,

$$y = f_d sin\frac{k}{f_d}x \tag{3.14}$$

Using this equation Jakes distributed number can be generated from uniform number generator.

In the last chapter a possibility was introduced that the most successful DFT systems may not perform very well in some channel conditions. Main problem of such systems is their high sidelobes which give rise to ICI in doppler dispersive channels. Multicarrier techniques discussed till now are normally used in cables and broadcasting, where fading and frequency dispersion are not present or at least are not so pronounced to be considered. These systems experienced negligible doppler dispersion and hence are least concerned with the high sidelobes of DFT based multicarrier systems. But for the doppler dispersive channels high sidelobes can no more be ignored. To reduce sidelobes we can use shaped cyclic prefix[2]. This will reduce far-out sidelobes considerably but gives a little reduction in close-in sidelobes[8].

In serious doppler dispersions these sidelobes may still produce considerable interference. Few other techniques may be used to reduce it further[8], e.g.-

- **Frequency domain spreading:** This method uses frequency response partial coding and polynomial cancellation.
- **Discrete wavelet multitone modulation:** FFT of earlier system can be replaced by Discrete Wavelet Transform. This will be called as DWMT modulation.
- **Pulse shaping:** We can use other pulse shapes rather than using rectangular pulse shape, to reduce sidelobes

Hence different types of multicarrier systems can be developed depending upon which one of the above sidelobe reduction techniques is used. Pulse shaping will be focus of attention in this thesis.

3.2 Pulse shape design

Pulse shaping is done to reduce sidelobes. However this has a limitation that pulse which decreases sidelobes, spreads in time domain making it sensitive to the delay dispersion. Hence the objective of pulse design is to find a compromise between ISI and ICI in order to minimize total interferences. Proceeding with the general analysis of the pulse shape to be used in multicarrier systems, following condition can be derived.

3.2.1 Orthogonality Condition

Let Ψ_{pq} be the basis of transmit signal, i.e. p^{th} symbol at q^{th} carrier. c_{pq} will be transmitted as $c_{pq}\Psi_{pq}(t)$, where $\Psi_{pq}(t) = g(t - pT_s)e^{j2\pi q\Delta f_c t}$

Hence transmitted signal can be represented as,

$$y(t) = \sum_{q=0}^{N_c-1} \sum_{p=-\infty}^{\infty} c_{pq}\Psi_{pq}(t) \tag{3.15}$$

To receive n^{th} symbol at k^{th} carrier, the transmitted signal will be convolved with $\psi^*_{nk}(t)$ i.e. $g^*(t - nT_s)e^{-j2\pi k\Delta f_c t}$. The output will be,

$$r(t) = \sum_{q=0}^{N_c-1} \sum_{p=-\infty}^{\infty} \int_{-\infty}^{\infty} c_{pq}\Psi_{pq}(\tau)\Psi^*_{nk}(t-\tau)d\tau \tag{3.16}$$

To get zero ISI and ICI it should give,

$$r(0) = c_{nk} \tag{3.17}$$

Hence pulses should satisfy the following orthogonality condition,

$$\int_{-\infty}^{\infty} \Psi_{pq}(t)\Psi_{nk}^{*}(-t)dt = \delta_{np}\delta_{kq} \tag{3.18}$$

where,

$$\delta_{ni} = \begin{cases} 1 & n = i \\ 0 & \text{elsewhere} \end{cases} \tag{3.19}$$

Equation 3.18 can be written as,

$$\int_{-\infty}^{\infty} g(t - pT_s)g^{*}(t - nT_s)e^{j2\pi(q-k)\Delta f_c t}dt = \delta_{np}\delta_{kq} \tag{3.20}$$

Equation 3.20 can be transformed in frequency domain as-

$$\int_{-\infty}^{\infty} G(f)G^{*}(f - (q-k)\Delta f_c)e^{j2\pi(n-p)T_s f}df = \delta_{np}\delta_{kq} \tag{3.21}$$

Hence any pulse shape to be used in multicarrier must satisfy above condition to give zero ISI and ICI.

3.3 Various orthogonal pulse shapes

If for any pulse shape satisfying above condition $g(t) = g^{*}(t)$, it is called to be orthogonal pulse shape. Because in this condition the basis functions for transmission and reception belong to the same family and are orthogonal to each other. Few examples can be seen here,

3.3.1 Rectangular Pulse

This is the most common pulse shape used in DFT based multicarrier systems. This pulse shape can be formulated as i.e. $g(t) = g^{*}(t) = 1$ for $\frac{T_s}{2} \leq t \leq \frac{T_s}{2}$ Hence for this equation 3.20 simplifies to the following condition

$$\int_{0}^{T_s} \left(cos2\pi\frac{(q-k)}{T_s}t + jsin2\pi\frac{(q-k)}{T_s}t \right) dt = \delta_{kq} \tag{3.22}$$

where carrier spacing $\Delta f_c = \frac{1}{T_s}$. This result can be extended for $\Delta f_c = \frac{n}{T_s}$ where $n = 1, 2, 3...$ This condition can easily be proved for $(q-k)$ as integer. For $n = 1$ it will achieve maximum

3.3.2 Nyquist Pulse

If subcarriers are alloted disjoint spectra and each individual spectrum is flat, this pulse corresponding to it can be formulated as $G(f) = G^*(f) = 1$ for $\frac{-\Delta f_c}{2} \leq f \leq \frac{\Delta f_c}{2}$, where $G(f)$ is fourier transform of $g(t)$ and $\Delta f_c = \frac{1}{T}$. For this equation 3.21 simplifies like this,

$$\int_0^{\frac{1}{T_s}} (cos2\pi(n-p)T_s f + jsin2\pi(n-p)T_s f)\, df = \delta_{np} \tag{3.23}$$

Above condition also can be extended for $\Delta f_c = \frac{n}{T_s}$, where $n = 1, 2, 3...$ For $n = 1$ it will achieve maximum efficiency. This condition again can easily be proved for $(n-p)$ as integer. For $n = 1$ it will achieve maximum spectral efficiency.

For practical implementation in simulation this pulse has been truncated and thus $g(t) = g^*(t) = \frac{sin\pi t}{\pi t}$ for $-4T_s \leq t \leq 4T_s$ and zero otherwise. Because of truncation it has some ringing in frequency domain.

3.3.3 Raised Cosine Pulse

This pulse is defined as $g(t) = F^{-1}(\sqrt{H(f)})$ where $H(f)$ is raised cosine spectrum. It can be formulated as-

$$H(f) = \begin{cases} \frac{1}{2W}, & 0 \leq |f| < f_1 \\ \frac{1}{4W}\left\{1 - sin\left[\frac{\pi(|f|-W)}{2W-2f_1}\right]\right\}, & f_1 \leq |f| < 2W - f_1 \\ 0, & |f| \geq 2W - f_1 \end{cases} \tag{3.24}$$

where $\alpha = 1 - \frac{f_1}{W}$ and $W = \frac{1}{2T_s}$. Checking the orthogonality condition for this pulse, it can be seen that putting $n = p$ in equation 3.21 reduces L.H.S. to the area of multiplication of the spectrum of the pulse and its version shifted by $(q-k)\Delta f_c$. It can be seen that equation is not satisfied for $\Delta f_c < \frac{1+\alpha}{T_s}$ It can be proved that equation 3.21 is actually satisfied for $\Delta f_c \geq \frac{1+\alpha}{T_s}$. For $\alpha = 1$ this pulse is said to be having *full cosine roll off* and equation 3.24 simplifies to-

$$H(f) = \begin{cases} \frac{T_s}{2}[1 + cos(\pi f T_s)], & 0 < |f| < \frac{1}{T_s} \\ 0, & |f| \geq \frac{1}{T_s} \end{cases} \tag{3.25}$$

This pulse does not satisfy orthogonality condition for $\Delta f_c T_s = 1$ but satisfies it for $\Delta f_c T_s = 2$. Hence it can achieve only half of the spectral efficiency.

3.3.4 Hermite Pulse

This pulse shape was proposed in [5]. This pulse was not designed for full spectral efficiency. This satisfies orthogonality condition for $\Delta f_c T_s = 2$ and thus achieves half of the spectral efficiency. Shape of this pulse was has been given in figure 3.4. This pulse was proved better

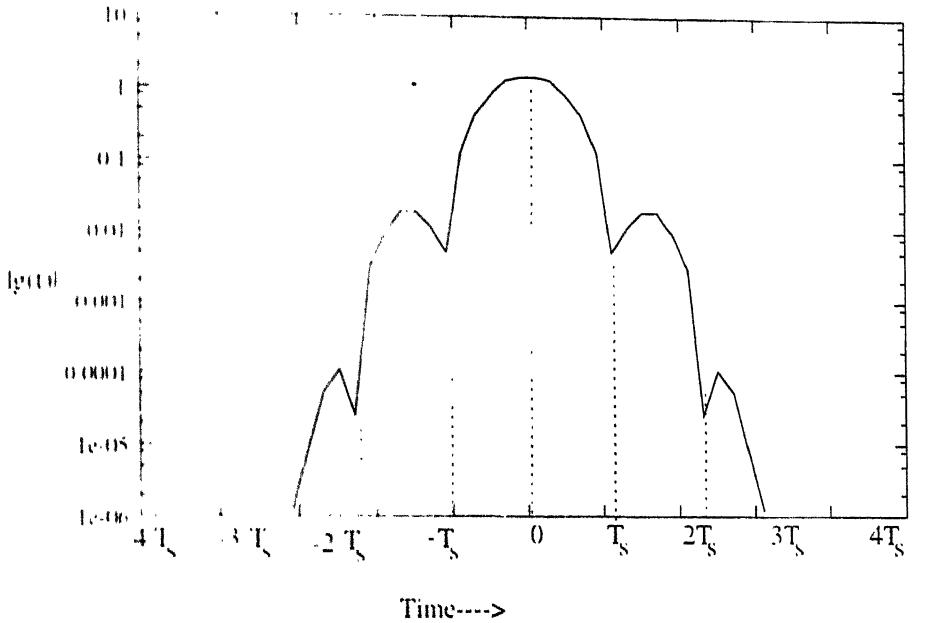

Figure 3.4: Hermite pulse

than Raised Cosine having full cosine roll off.

3.4 Non-orthogonal Pulses

The pulses discussed till now belong to the orthogonal family. In [6] the possibility of non-orthogonal pulses was introduced in order to combat ISI and ICI better. This was based on the concept of using mismatched filter. Though because of use of mismatched filter it does not maximize SNR and hence does not show good performance for AWGN channels. But in mobile environments the performance of system rarely depends upon only AWGN performance. It widely depends upon ISI and ICI cancellations as well.

Here $g(t) \neq g'(t)$. $g'(t)$ can be denoted as $\gamma(t)$. Both the pulses can be called dual of each other. As we have got two families, every basis of one is orthogonal with the one in other but not from the same family. Hence $g(t)$ and $\gamma(t)$ are said to be biorthogonal. These also satisfy orthogonality condition for $\Delta f_c T_s = 2$.

From the above two families if one is used for transmission, other one will be used for reception. As can be seen that $q(t)$ has a longer time support than $s(t)$, it is suggested to use $s(t)$ at the mobile terminals and $q(t)$ at stationary terminals.

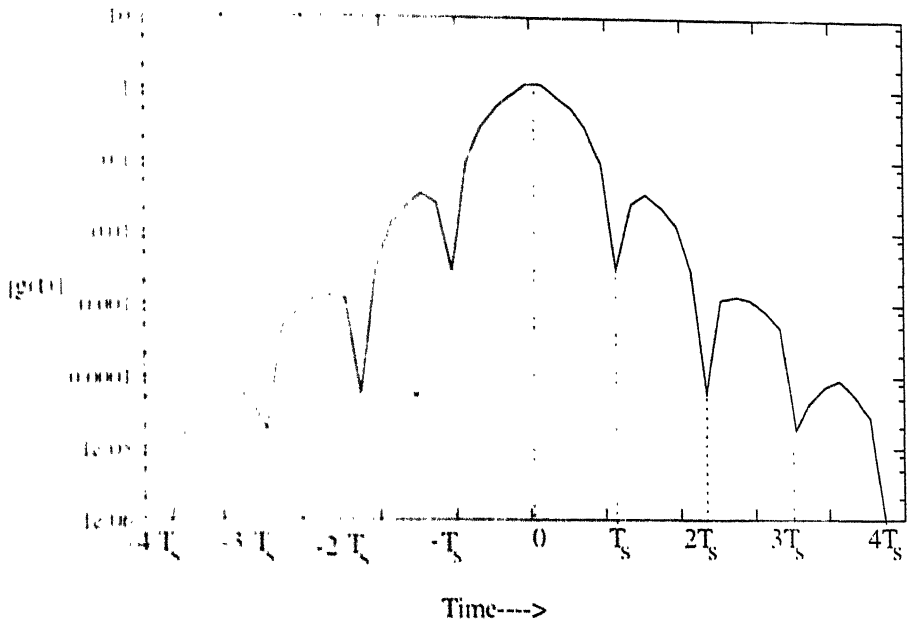

Figure 3.5: Non-orthogonal pulse, $g(t)$

These pulses were compared with the Hermite pulses in [6] and were proved giving better performance.

Time domain shaping came to reduce sidelobes in frequency domain. But as a signal can not be defined in both the domains simultaneously, decreasing sidelobes in frequency domain will spread the pulse in time domain making it sensitive to the delay dispersion. To analyze the pulse in both the domains together Ambiguity function[10] can be used.

3.5 Ambiguity function

Ambiguity function represents the response of the matched filter to the signal for which it is matched as well as to delay-doppler-shifted (mismatched) signals[10]. Output of the matched filter $s(t)$ is,

$$s(\tau)|_{\tau=0} = \int_{\infty} g(t)g^*(\tau - t)dt \tag{3.26}$$

Hence,

$$output = \int_{-\infty}^{\infty} g(t)g^*(-t)dt \tag{3.27}$$

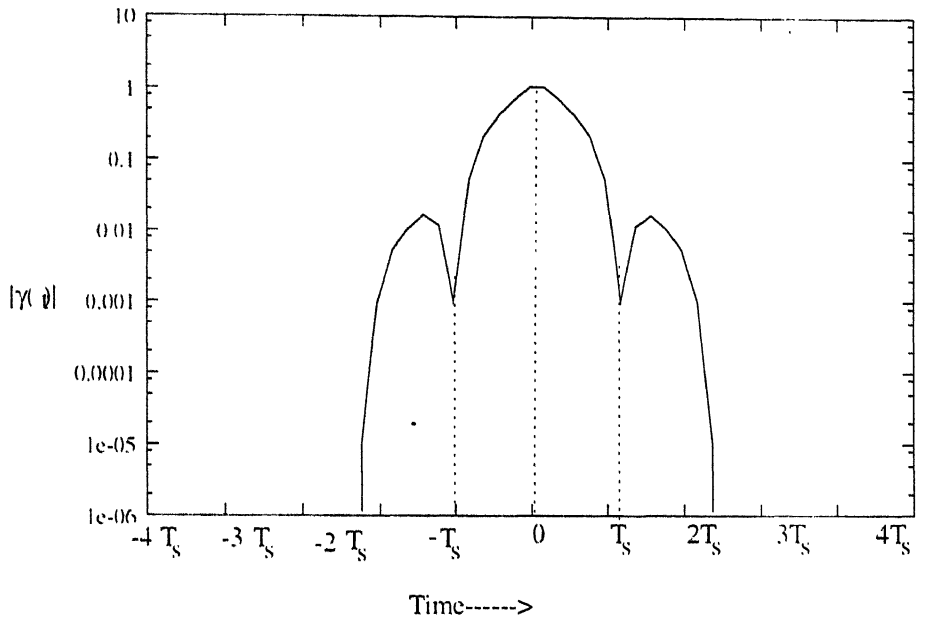

Figure 3.6: Dual of pulse $g(t)$, $\gamma(t)$

Then output of the filter to a mismatched signal shifted by τ in time and f in frequency will be,

$$A(\tau, f) = \int_{-\infty}^{\infty} g(t)g^*(\tau - t)e^{-j2\pi ft}dt \tag{3.28}$$

Generally pulse shape $g(t)$ is such that $g(t) = g(-t)$ then,

$$A(\tau, f) = \int_{-\infty}^{\infty} g(t)g^*(t + \tau)e^{-j2\pi ft}dt \tag{3.29}$$

$|A(\tau, f)|^2$ is called Ambiguity function of $g(t)$.

3.5.1 Analysis of pulse shapes using Ambiguity Function

Consider the family of orthogonal basis function Ψ_{nk}, $n = -\infty.. - \infty$. $k = 0, 1, .., (N_c - 1)$ where $\Psi_{nk} = g(t - nT_s)e^{-j2\pi kft}$. Then these should satisfy orthogonality condition as given in equation 3.18

Left hand side of the equation 3.18 can be expanded as,

$$\int_{-\infty}^{\infty} \Psi_{pq}(t)\Psi^*_{nk}(t)dt = \int_{-\infty}^{\infty} g(t)g^*(t + iT_s)e^{-j2\pi l\Delta fct}dt \tag{3.30}$$

where, $i = p - n, l = k - q$. Right hand side of equation 3.30 is the Ambiguity function

sampled at $pT_s, q\Delta f$. Hence

$$\int_{-\infty}^{\infty} \Psi_{pq}(t)\Psi_{nk}^*(t)dt = A(iT_s, l\Delta f) \tag{3.31}$$

From equations 3.31 and 3.18 it can be seen that $A(0,0) = 1$. Received signal can be written as follows

$$r(\tau)|_{\tau=0} = \sum_{q=0}^{N_c-1} \sum_{p=-\infty}^{\infty} \int_{-\infty}^{\infty} c_{pq} g(t - pT_s) e^{j2\pi q\Delta f_c t} g^*(t - nT_s - \tau) e^{j2\pi k\Delta f_c(t-\tau)} \tag{3.32}$$

Representing n^{th} symbol received on k^{th} carrier as $r(nT_s, k\Delta f)$ above equation can be represented in terms of Ambiguity function as,

$$r(nT_s, k\Delta f) = \sum_{q=0}^{N_c-1} \sum_{p=-\infty}^{\infty} c_{pq} A((p-n)T_s, (q-k)\Delta f) \tag{3.33}$$

where c_{pq} is p^{th} symbol transmitted on q^{th} carrier. In ideal orthogonality conditions above equation will simplify to

$$r(nT_s, k\Delta f) = c_{nk} A(0,0) \tag{3.34}$$

Hence signal to interference noise ratio (SINR) can be lower bounded[2] as,

$$SINR \geq \frac{A(0,0)}{\sum_{q=0}^{N_c-1} \sum_{p=-\infty}^{\infty} A((p-n)T_s, (q-k)\Delta f) - A(0,0)} \tag{3.35}$$

Similarly SINR for doubly dispersive channel having delay and doppler dispersion as T_d and f_d can be lower bounded as

$$SINR \geq \frac{A(0,0)}{\sum_{q=0}^{N_c-1} \sum_{p=-\infty}^{\infty} A((p-n)T_s + T_d, (q-k)\Delta f + f_d) - A(0,0)} \tag{3.36}$$

Above bound can be used to compare different pulses.

3.5.2 Computation of Ambiguity Function

As given in equation 3.29 Ambiguity function is defined as

$$A(\tau, f) = \int_{-\infty}^{\infty} g(t) g^*(t-\tau) e^{-j2\pi ft} dt \tag{3.37}$$

This can be viewed as fourier transform of $g(t)g^*(t-\tau)$, with τ as a constant. Both $g(t)$ and $g^*(t)$ have been implemented as impulse response of 48 tap FIR filters in simulation. For the sake of computation of ambiguity diagram by FFT, $g(t)$ and $g^*(t)$ has been extended to 64 tap adding 8 taps of zero value each side. Then 64 point FFT of the product $g(t)g^*(t-\tau)$ has been taken varying the value of τ.

[2]Because neighboring carriers may not necessarily have different symbol than one to be decoded.

3.6 Simulation Model

To analyze the performance of different pulse shapes a simulation model has been implemented. Pulse shaping filter has been implemented as 48 tap finite impulse response (FIR) filter. Binary phase shift keying scheme has been used to transmit bits over channel. Carriers have been separated by multiplying the output of FIR filter with $cos(2\pi n \Delta f_c t)$, where $n = 0, 1, 2, 3...$ for different carriers. $\Delta f_c = \frac{1}{T_s}$ has been taken to get maximum spectral efficiency. Only one carrier has been demodulated for BER observations assuming all the carriers similar. Fixed loading has been used and white noise has been taken. Channel has been modeled as doubly dispersive having exponential power-delay profile, i.e. power of n^{th} path P_n delayed by T_d is $P_0 e^{\frac{-(T_d - T_0)}{\tau_{max}}}$, where T_0 is the delay of earliest reaching path and has been taken zero. P_0 is the power of a path coming with T_0 delay. The sum of the total power of all the paths is normalized. Doppler spread has been modeled as Jakes spectrum represented as $\frac{1}{\sqrt{1-(\frac{f}{f_d})^2}}$, where f_d is maximum doppler dispersion. In simulation, Jakes spectrum have been produced by Jakes distributed random doppler shifts. A random number having probability density function as Jakes spectrum has been generated starting from uniform number generator. This generation is discussed in next section. Channel has been assumed constant for one symbol duration. Step wise process can be understood from flow chart in figures 3.7 and 3.8.

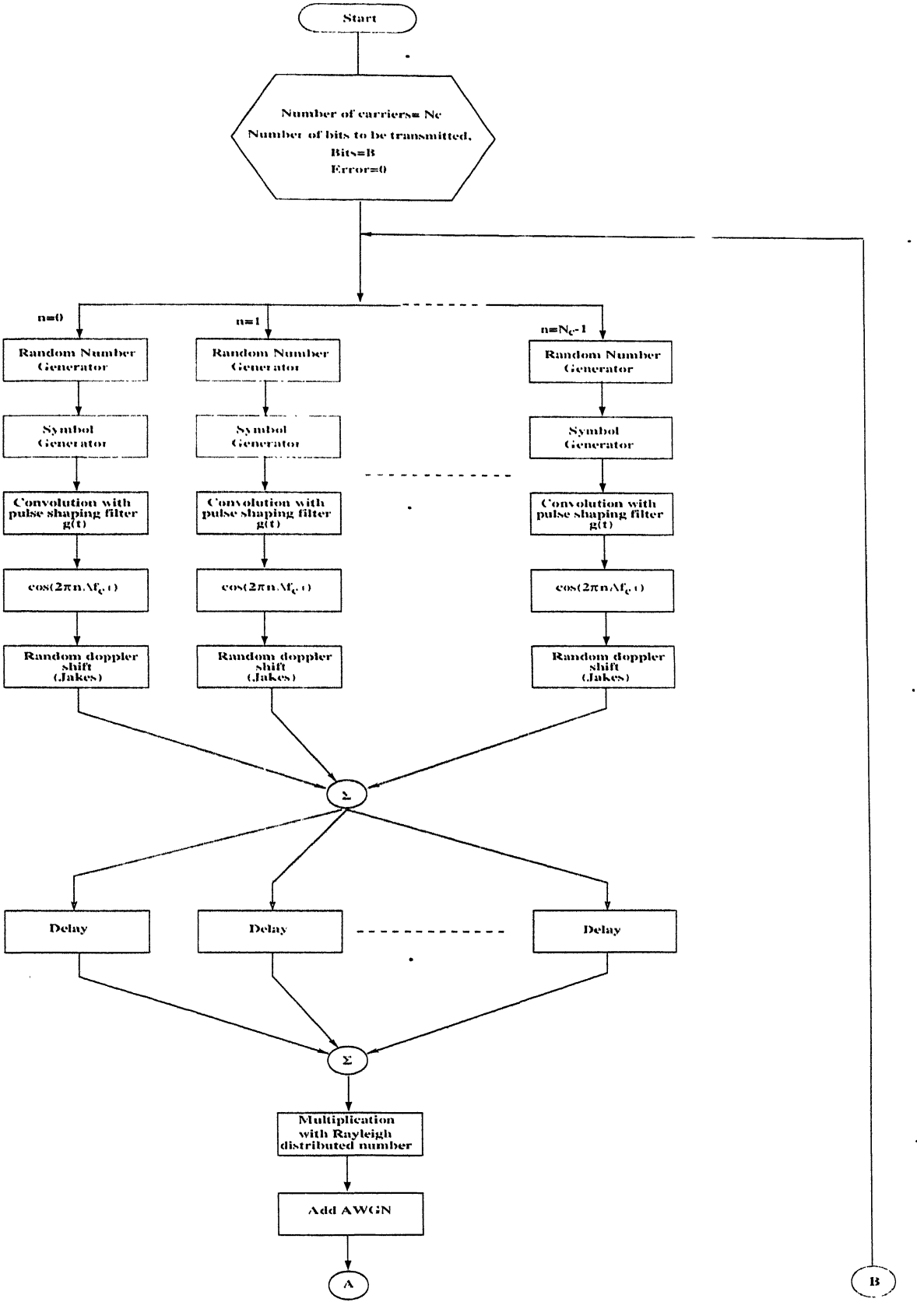

Figure 3.7: Flow chart of simulation model

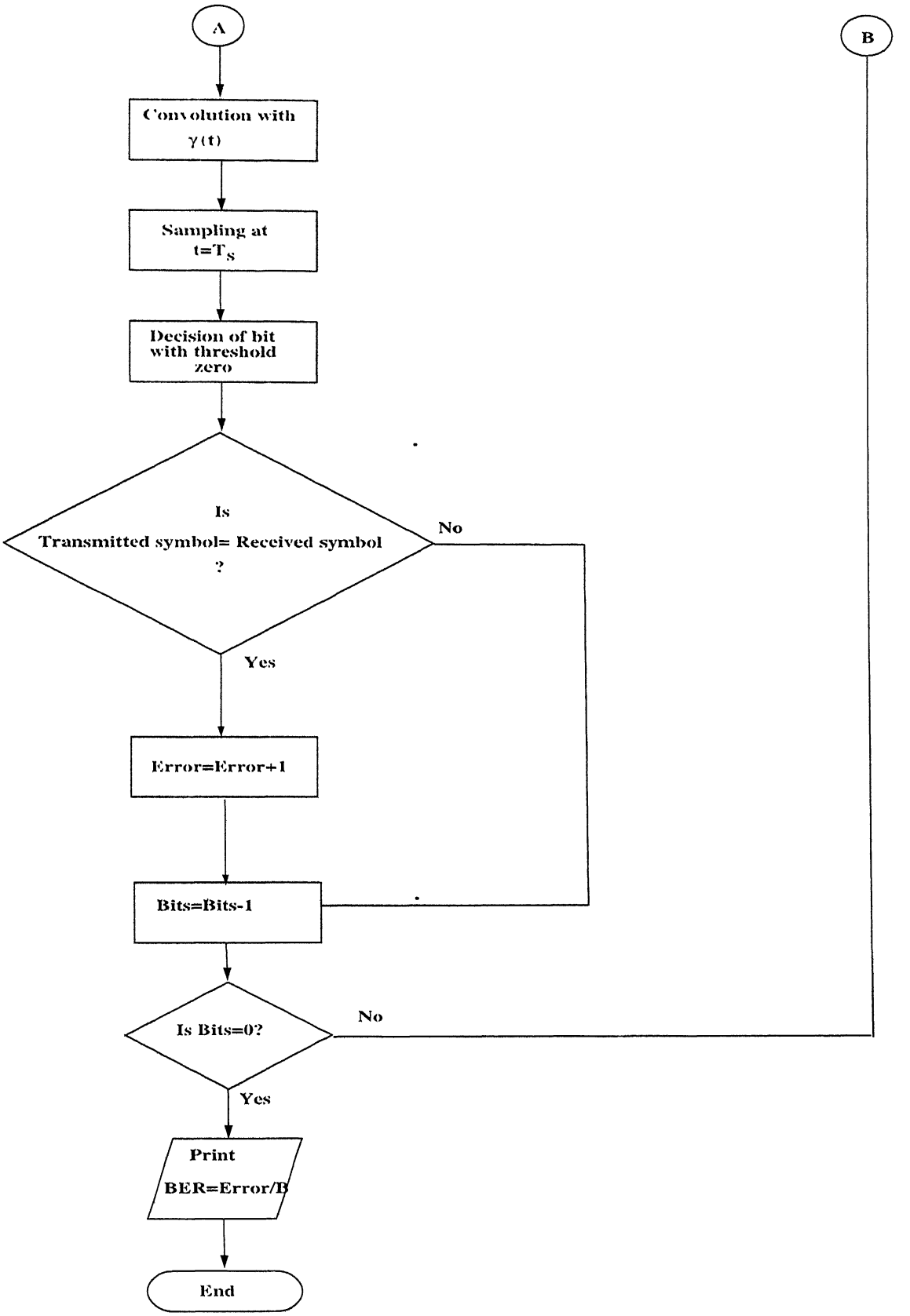

Figure 3.8: Flow chart (cont'd.)

Chapter 4

Results and Discussion

Pulse shapes in doubly dispersive channels can be qualitatively analyzed by their ambiguity diagram.

4.1 Qualitative analysis by ambiguity diagrams

Observing the ambiguity diagrams of all the pulses we can analyze them as follows-

4.1.1 Rectangular Pulse

Rectangular pulses do not overlap for two symbols. Hence in the case of delay dispersion $< T_s$, only neighboring symbols interfere with one symbols.

These properties can be seen by ambiguity diagram (see figure 4.1). This is zero after +1 and -1 in time axis which represents that a symbol away by more than one symbol period does not interfere. But in frequency axis decrement is sluggish representing high sidelobes and showing the possibility of high ICI in doppler dispersion cases.

4.1.2 Nyquist Pulse

In time domain this pulse is what rectangular pulse is in frequency domain and in frequency domain this pulse corresponds to rectangular shape, what rectangular pulse was in time domain. Hence effects of delay and doppler dispersions are just reverse than in case of rectangular pulse. Carrier spectra do not overlap and hence in case of doppler dispersion

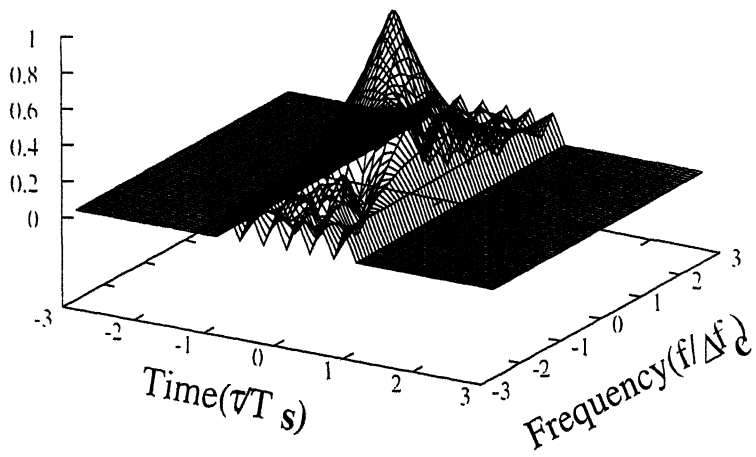

Figure 4.1: Ambiguity function of square pulse

$< \Delta f_c$, only neighboring carriers interfere to a carrier. The same can be examined by ambiguity diagram (see figure 4.2). This is zero after +1 and -1 in frequency axis which represents that a carrier away by more than Δf_c does not interfere. But in time axis the decrement is sluggish showing that it is sensitive towards delay dispersion.

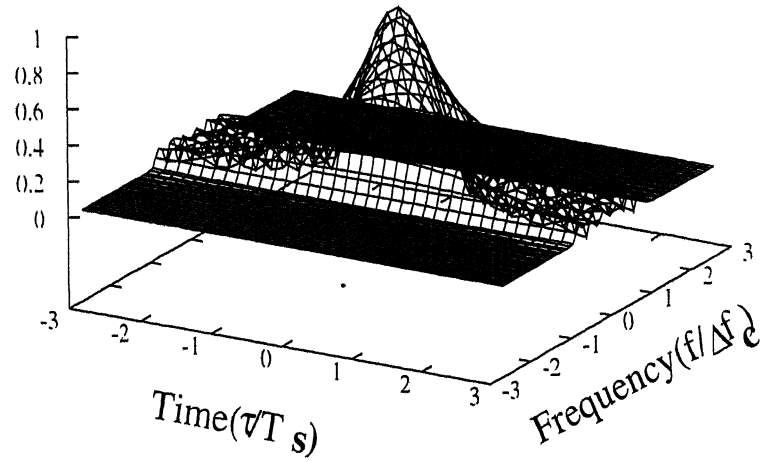

Figure 4.2: Ambiguity function of Nyquist pulse

4.1.3 Raised Cosine Pulse

Ambiguity function for raised cosine pulse having full cosine roll off has been given in figure 4.3. This can be observed that it is zero after +2 and -2 not after +1 and -1. Hence a carrier will be interfered by the carriers away by $\frac{1}{T_s}$ but will have no interference by the

carriers away by $\frac{2}{T_s}$. That we have already seen this pulse satisfies orthogonality condition for $\Delta f_c = \frac{2}{T_s}$ not for $\Delta f_c = \frac{1}{T_s}$.

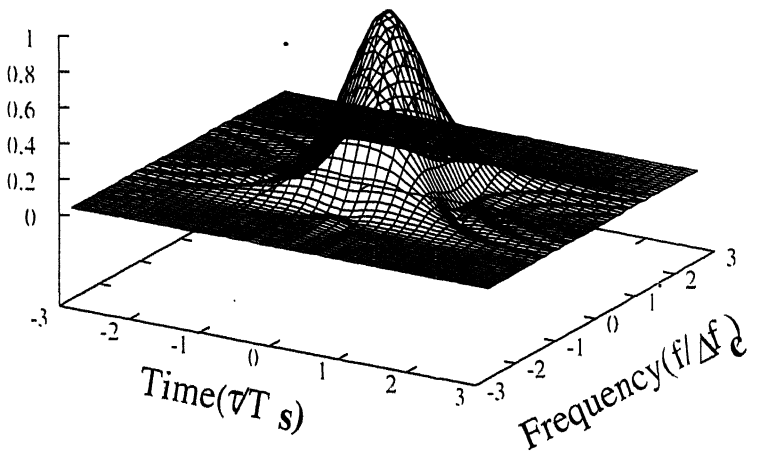

Figure 4.3: Ambiguity function of Raised cosine pulse

4.1.4 Hermite and Non-orthogonal Pulses

Ambiguity functions of these pulses are somewhat similar to that of raised cosine pulse (see figures 4.4 and 4.5). We can observe a bit of more dispersion in frequency domain but the values after +2 and -2 are very small and hence it is difficult to draw a definite conclusion from it. Simulations have been used to compare their performance.

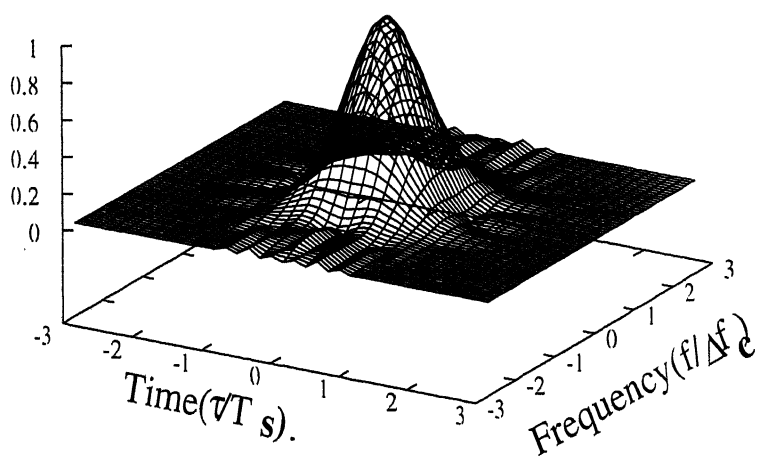

Figure 4.4: Ambiguity function of Hermite pulse

This has been seen that only rectangular and Nyquist pulses achieve maximum spectral

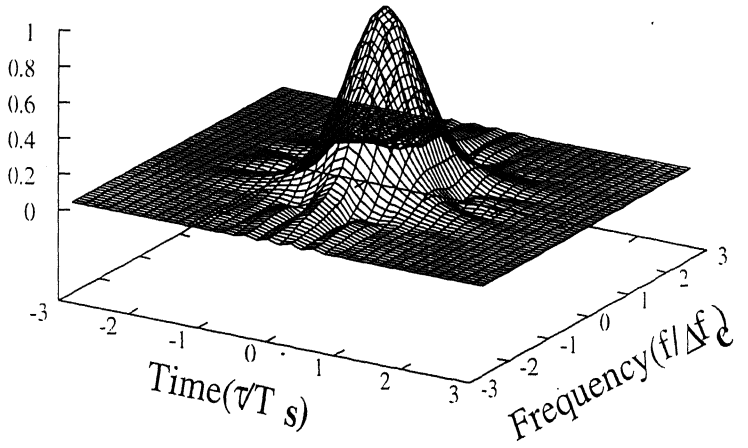

Figure 4.5: Ambiguity function of Non-orthogonal pulse

4.2 Comparison of pulses in delay and doppler dispersive channel

It can be observed from figures 4.6 and 4.7 that for lower dispersions rectangular pulse and Nyquist pulse shows much better performance than others. This is probably because of the fact that only these two pulses show orthogonality for full spectral efficiency which is the case taken for simulations. For delay dispersion of more than 0.2 the performance of Nyquist pulse becomes worse because it has slowly decreasing values. For doppler dispersion above 0.01 rectangular pulse starts showing worse which is justified because of high sidelobes. For doppler dispersion above 0.1 Nyquist pulses also are no good than others. Hence till the value of delay dispersion exceeds 0.2, and doppler dispersion exceeds 0.1, the compromise with spectral efficiency is not needed and use of rectangular and Nyquist pulses can be continued. Above conclusion can again be seen in figures 4.8 and 4.9 that for doppler dispersion of 0.1 rectangular pulse proves better till the delay dispersion of 0.5 and for delay dispersion of 0.2 Nyquist pulse proves better till the doppler dispersion of 0.2.

Now it can be seen by an example that the dispersion values where both of these pulses giving full spectral efficiency are valid for normal data rate.

Suppose $2Mbps$ data rate has to be transmitted and bandwidth alloted is $5Mhz$. as is the case for third generation mobile systems. Typical mobile environment for urban areas hardly show delay dispersion of more than $20\mu s$ and doppler dispersion of more than $250Hz$

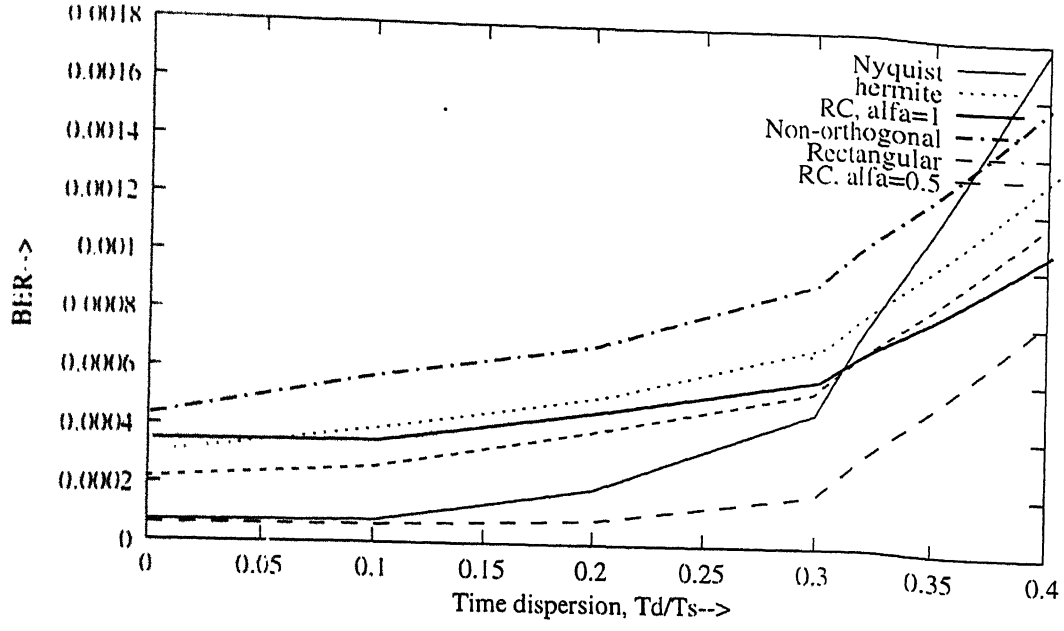

Figure 4.6: Comparison of different pulses in delay dispersive channel

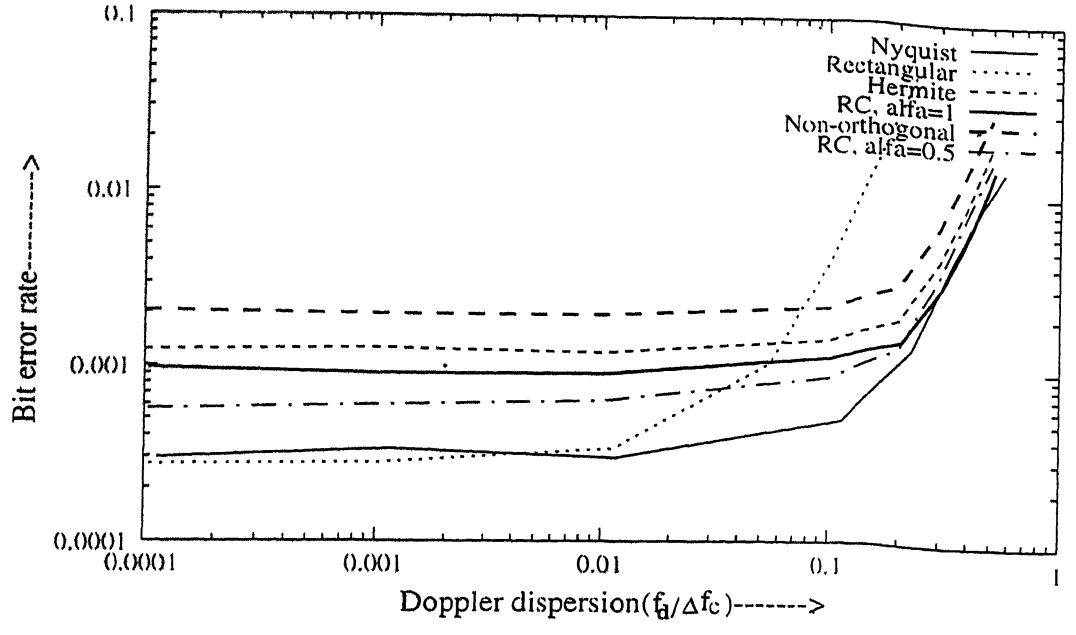

Figure 4.7: Comparison of different pulses in doppler dispersive channel

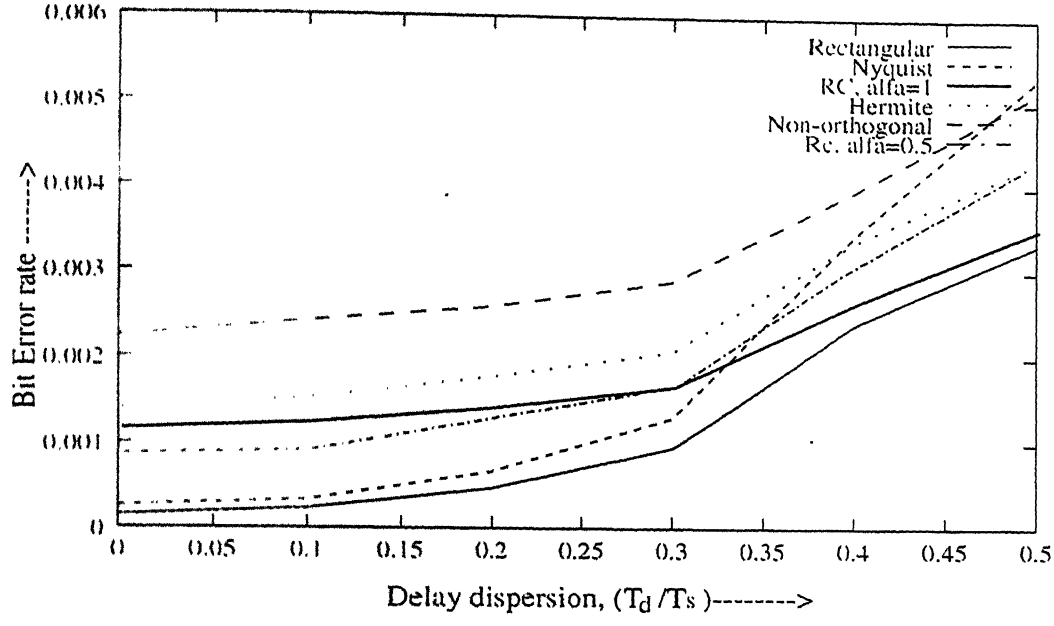

Figure 4.8: Comparison of different pulses in doubly dispersive channel, doppler dispersion is fixed at 0.1

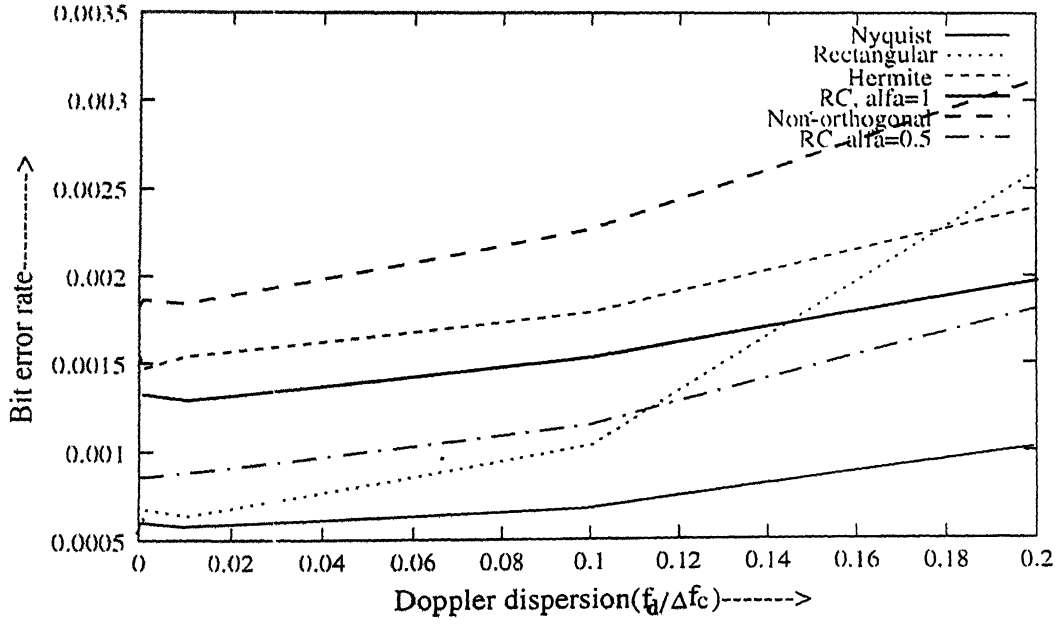

Figure 4.9: Comparison of different pulses in doubly dispersive channel, delay dispersion is fixed at 0.2

(see [13] and [14]). Actually these values themselves are highly pessimistic. If we use 500 carriers, then for the above case symbol period $T_s = 250\mu s$ and $\Delta f_c = 50kHz$. Hence the delay dispersion $\frac{f_d}{f_c} = 0.08$ and doppler dispersion $\frac{f_d}{\Delta f_c} = 0.025$. These values of dispersion correspond to the region where rectangular and Nyquist pulses are far better than others.

4.3 Conclusion

After examining these pulses we see that if high spectral efficiency is desired, rectangular and Nyquist pulses can be used as these satisfy orthogonality condition for full spectral efficiency. Further they achieve lesser bit error rate for moderate dispersions. However between these two, rectangular pulse is more suitable for channels having large delay dispersion, while Nyquist pulse is more suited for channels having large doppler dispersion. Rectangular pulse allows the use of guard interval, while Nyquist pulse allows the use of guard band. However, for high dispersion channels these pulses are no good than other lower spectral efficiency pulses. For half spectral efficiency Hermite pulses can be considered which are well localized and can combat ISI and ICI equally. Further, again for half spectral efficiency non-orthogonal pulses can combat ISI and ICI better than Hermite pulses though they do not maximze SNR. For higher data rate or more dispersive channels these pulses can be considered.

Bibliography

[1] R.W. Chang, "Synthesis of bandlimited orthogonal signal for multichannel data transmission." *Bell Syst. Tech. Journal*, vol. 45, pp 1775-1796, 1996.

[2] S. B. Wienstein and Paul M. Ebert, "Data transmission by frequency Devision Multiplexing using the Discrete Fourier transform." *IEEE trans. comm. tech.* vol. COM-19. No. 5. pp 628-634. Oct-1971.

[3] John A.C. Bingham, "Multicarrier modulation for data transmission: An idea whose time has come." *IEEE Comm. Mag.*, pp. 5-14[1], May-1990

[4] M. L. Doelz, E. T. Heald and D. L. Martin, "Binary data transmission techniques for linear systems." Proc. IRE, pp. 656-661, May 1957

[5] Ralf Hass and Jean-Claude Belfiore, "A time frequency well localized pulse for multiple carrier transmission." *Wireless Personal Communications*, vol. 5, pp. 1-18, 1997

[6] Werner Kozek, "Nonorthogonal pulse shapes for multicarrier communication in doubly dispersive channels." *IEEE Journal on selected areas in comm.*, vol. 16, No. 8, pp. 1579-1589. Oct 1998

[7] J.G. Proakis, "Digital Communication *third edition*," *McGraw-Hill Publication* 1995.

[8] John A.C. Bingham, "ADSL, VDSL and Multicarrier Modulation," *Wiley-Interscience Publication*, 2000.

[9] Richard Van Nee and Ramjee Prasad, "OFDM for wireless multimedia communications." *Artech House Publishers* 2000

[1] A printing mistake may be noticed that Page no. 11 comes after page no. 8, though article is continued.

[10] Merrill I. Skolnik. "Introduction to Radar Systems *Second Edition*," *McGraw Hill Publication* 1981.

[11] William C. Jakes.Jr., "Microwave Mobile Communication," *Wiley Interscience Publication* 1974.

[12] William C. Y. Lee. "Mobile Communication Engineering: Theory and Applications." *Second Edition.*

[13] Raymond Steele and Lajos Hanzo, "Monile Radio Communications," *Secon Edition. Second and Third generation Cellular and WATM Systems, IEEE Press* 1999.

[14] Jhong Sam Lee and Leonard E. Miller, "CDMA Systems Engineering Handbook." *Artech House* 1998.

[15] Marvin K. Simon and Mohamed-Slim Alouini, "Digital Communication over Fading Channels. *A unified approach to performancce analysis*," *Wiley-Interscience* 2000.

A133902

Date Slip

This book is to be returned on
he date last stamped.